Journal of Non-Crystalline Solids 356 (2010) 3019–3025

Contents lists available at ScienceDirect

Journal of Non-Crystalline Solids

journal homepage: www.elsevier.com/ locate/ jnoncrysol

Crystallization during processing of nuclear waste glass

Pavel Hrma

Pacific Northwest National Laboratory, Richland, Washington, United States

ARTICLE INFO

Article history:
Received 1 October 2009
Received in revised form 22 March 2010
Available online 31 July 2010

Keywords:
Crystallization;
Nonequilibrium conditions;
Nuclear waste glasses;
Agglomeration;
Settling

ABSTRACT

Under typical glass-processing conditions, crystals nucleate, grow, and dissolve in a nonuniform temperature field in a melt subjected to deformation and flow. Using examples of the results obtained on nuclear waste glasses, this paper describes various phenomena associated with crystallization under non-static conditions, such as crystal formation during batch melting, crystal settling at the melter bottom, and crystal precipitation during glass cooling, including its impact on glass corrosion resistance.

1. Introduction

Almost all commercial glasses, all waste glasses and geological glasses, and many specialty glasses are multicomponent. Crystals that grow or dissolve in such glasses have a different composition from the matrix glass, and they often grow and dissolve at a changing temperature in a moving melt, or while moving through the melt by buoyancy.

Nuclear waste glasses are outstanding examples of multicomponent glasses. They contain a majority of the chemical elements of the periodic table, and their design and processing provide a plentiful opportunity for crystallization, which is allowed as long as it does not impair the chemical durability, the sole measure of waste glass quality. For the processing and storage economy, the waste fraction in the glass is typically as high as the processing and product quality constraints allow. Because the waste components are usually prone to crystallization and the final product is formed into large bodies in which the internal portion of the glass cools slowly, nuclear waste glasses may contain a variety of crystalline forms.

Though this paper is based on studies undertaken with glasses designed for the vitrification of nuclear wastes stored at Hanford, the features covered are typical, in many aspects, also for glasses industrially processed or made by nature.

Section 2 briefly describes the batch-to-glass conversion process, in which initially crystalline materials turn amorphous. Sections 3 and 4 review the role of the phase equilibria and crystal nucleation in multicomponent glasses. Section 5 focuses on the nonisothermal kinetics of crystal growth and dissolution when solid and liquid phases are in mutual motion. Section 6 informs about the effects of crystallization on glass processing and on the chemical durability of the glass. Two "exotic" phenomena: the dendritic growth and self-organized precipitation associated with a propagating temperature gradient, are mentioned in Sections 7 and 8.

2. Batch-to-glass conversion

Crystals can occur at any stage of glass making. As described in various papers and reviews [1–5], both commercial and waste glasses are usually produced from crystalline precursors. Crystalline batch materials are of two types: ionic salts (carbonates, nitrates, sulfates, halides, etc.) and simple or complex oxides, hydroxides, or oxyhydrates (silica, silicates, iron oxide and hydroxide, alumina, etc.). Ionic salts melt early on heating, forming low-temperature eutectics. Carbonates and nitrates then react with boron oxide, silica, and other components, releasing copious amounts of gas, whereas sulfates and halides partly dissolve in the glass-forming melt, partly evaporate or decompose, and partly segregate. As these batch materials melt and dissolve, new intermediate crystalline phases may form and later dissolve.

Quartz is usually added as the source of silica, a major glass former. The size of its particles is of a crucial importance. Small particles (~5 μm) dissolve too early, producing a highly-viscous melt that tends to create foam [1]. When large quartz particles (>100 μm) dissolve, the silica-rich layers of melt around them impinge on each other, usually pushed by gas bubbles moving through the less viscous melt. This results in the formation of slowly dissolving clusters of several silica particles.

Alumina may form intermediate crystalline phases of nepheline or a sodalite type phase. Similarly, zirconia may first form zirconium silicate, sodium–zirconium silicate, or rare-earth zirconates before it fully dissolves in molten glass [6].

E-mail address: pavel.hrma@pnl.gov.

0022-3093/$ – see front matter © 2010 Elsevier B.V. All rights reserved.
doi:10.1016/j.jnoncrysol.2010.03.039

In batches with a large content of iron, a fraction of iron oxide and hydroxide may turn into hematite that turns to magnetite when Fe (III) begins to reduce to Fe(II) at higher temperatures. Magnetite extracts from the melt other spinel-forming oxides, such as NiO and Cr_2O_3, becoming a solid solution of magnetite, trevorite, chromite, and other simple spinels. As the temperature increases, spinel crystals eventually partly or fully dissolve in the glass-forming melt.

Fig. 1 displays dissolution of quartz with simultaneous formation and subsequent dissolution of spinel and sodalite [7].

Nuclear wastes typically contain oxides of noble metals Pd, Rh, and Ru. Their salts are initially a part of the ionic-salt melt from which they may precipitate in the form of metals or oxides and partly dissolve in the glass-forming melt. Needle-shaped crystals of RuO_2 do not redissolve in the melt and may interact with spinel [8] as seen in Fig. 2.

3. Phase equilibria

Crystallization and dissolution phenomena, whether occurring during the batch-to-glass conversion or during slow cooling of glass, proceed far from equilibrium. The distance from equilibrium (in the composition space) drives the process. The liquidus temperature (T_L) defines the equilibrium for the primary crystalline phase. Above T_L, crystals can only dissolve. Below T_L, crystals can either dissolve or grow depending on whether the melt is oversaturated or undersaturated with the crystalline material.

Though phase diagrams for mixtures of two or three components demonstrate that the T_L versus composition function is highly nonlinear, resembling a hilly landscape, for many types of glasses, especially those with many "crowded" components, the composition region of interest allows us to approximate glass properties, including T_L, as linear functions of mass or mol fractions. Hence, on a sufficiently narrow composition region, T_L can be approximated as [9–13],

$$T_L = \sum_{i=1}^{N} T_i x_i \tag{1}$$

where T_i is the i-th component coefficient, x_i is the i-th component mass or mole fraction (or the atomic fraction of the i-th ion), and N is the number of liquidus-affecting components. To measure the component coefficients, the experiments are often designed in such a way that a property (T_L) is measured for glasses with a component added to or removed from, one at a time, a centroid composition. Thus, four compositions usually suffice for each component to obtain a reliable value of T_i and to verify the assumption of linearity.

In the glasses formulated for Hanford nuclear waste, spinel is a common primary crystalline phase whose T_L is represented by a flat hypersurface in an N-dimensional composition space with N around 15, depending on the selection of spinel-affecting components. When

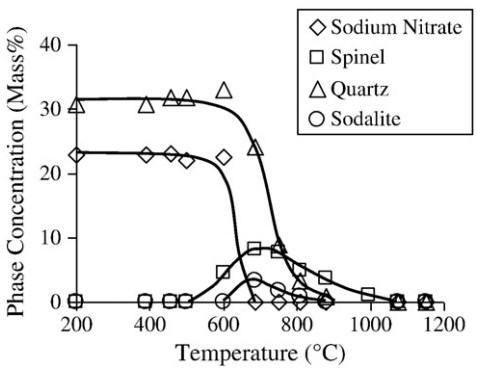

Fig. 1. Decomposition of sodium nitrate, dissolution of quartz, and formation and subsequent dissolution of spinel and sodalite during heating (at 4 °C/min) of a simulated nuclear waste batch.

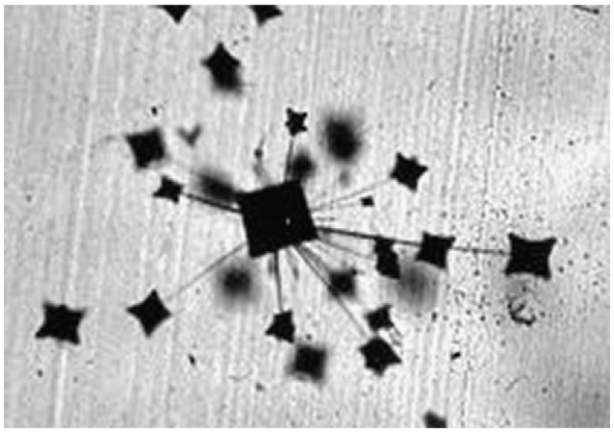

Fig. 2. Spinel crystals interacting with RuO_2 needles. The central spinel crystal is ~25 μm in size.

T_is for magnetite–trevorite–chromite spinel were expressed per mole fractions of cations, they correlated with the ionic potentials, $P_i = z_i/r_i$, where z_i is the ionic charge and r_i the ionic radius, forming two branches in the shape of Λ as seen in Fig. 3 [14]. This correlation allowed estimating T_is also for glass components for which the composition variation has not been performed. The only exceptions are Cr, Ni, and Mn, whose T_is do not fit the Λ pattern.

At a temperature below T_L, the equilibrium between the crystalline phase and the melt can be expressed in the form of a pseudo-binary mixture in which the crystalline material forms one component and the melt the other. An example of such a "binary" phase diagram [13] is shown in Fig. 4. The ideal-solution equation,

$$C_0 = C_{\max}\left\{1 - \exp\left[-B_L\left(\frac{1}{T} - \frac{1}{T_L}\right)\right]\right\} \tag{2}$$

where C_0 is the equilibrium mass fraction of crystalline phase in the mixture, and $C_{\max}$ and B_L are temperature-independent coefficients, represented the data well over a temperature interval of more than 300 °C below T_L. Since C_0 is a function of temperature, the degree of conversion, expressed as $\xi = (C_0 - C)/(C_0 - C_i)$ where C is the crystalline phase concentration, and the subscript i denotes the initial value, cannot be considered as an independent variable in nonisothermal processes (a commonly committed oversight) unless C_0 is nearly constant (at a temperature far bellow T_L).

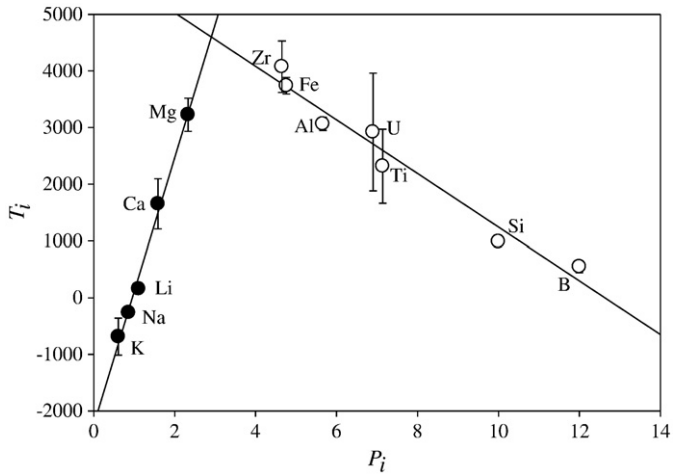

Fig. 3. Component coefficients of T_L, defined in Eq. (1) and expressed per atomic fractions, versus ionic potentials (P_i) of the prevailing redox state of the ions.

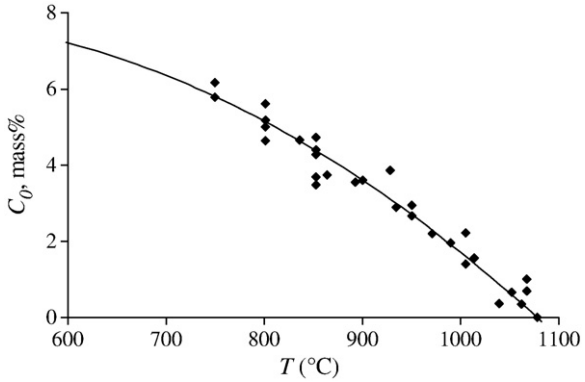

Fig. 4. Equilibrium concentration of spinel (in terms of mass%) in a simplified simulated nuclear waste glass. The line fitted to data represents the ideal solution Eq. (2).

4. Nucleation

In industrial glass processing, crystals nucleate on inhomogeneities, impurities, and surfaces and interfaces, such as bubbles, phase-separated liquid droplets, or other crystals. Certain crystals do not form unless the glass is first annealed at a lower temperature to generate nuclei. Other crystals, such as aegirine ($NaFeSi_2O_6$), form at a constant temperature only after some incubation time and thus may not form easily during cooling [15]. Structural elements of some crystals, such as nepheline, exist in the melt even above T_L [16]. Thus, nepheline precipitates rapidly as soon as the temperature drops below the liquidus [17]. Spinel exhibits a similar behavior. As Fig. 5 shows, ~10 crystals per mm^3 formed spontaneously below T_L in a waste glass [13]. When the melt was quenched to various temperatures below T_L, the number of spinel nuclei increased by orders of magnitude until it reached a maximum of ~10^8 crystals per mm^3 at ~500 °C.

Nucleation density determines the crystal size, a, by the relationship $a=(C/\zeta n_S\rho)^{1/3}$, where ζ is the shape factor, n_S is the crystal number density, and ρ is the crystal density. Thus, the smaller the number of crystals nucleated, the larger the crystals grow.

5. Crystal growth/dissolution rate

Both the growth rate and the dissolution rate of a crystal in a multicomponent glass are commonly controlled by diffusion. The diffusion flux at the interface is $j=\rho da/dt$, where t is the time, and ρ is the density. By the Fick's law, $j=-\rho D\ \partial C/\partial x|_{x=0}$, where D is the effective binary diffusion coefficient, and x is the distance from the interface. Alternatively, $da/dt=(D/\delta)\ (C_0-C_B)$, where δ is the diffusion boundary layer thickness, C_0 is the concentration of the crystalline material at the solid–melt interface (under common circumstances, the melt at the interface is saturated, and thus C_0 is the equilibrium concentration), and C_B is the concentration of the crystalline material in bulk. The mass transfer coefficient, h, is defined as $h=D/\delta$; hence, $da/dt=h(C_0-C_B)$. For simplicity, we have omitted secondary phenomena, such as the moving boundary, the impact of multicomponent diffusion on the composition at the interface, or the changing solid composition if the crystal is a solid solution.

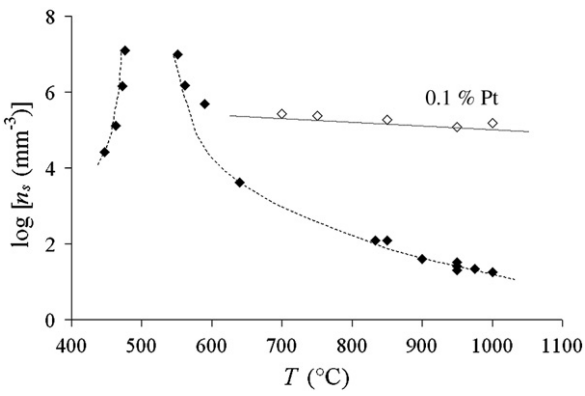

Fig. 5. The spinel nucleation density, n_S, versus temperature in a simplified nuclear waste glass without (solid points) and with an addition of 0.1 mass% of Pt (open points).

As the diffusion layers around growing crystals grow, they may eventually impinge at each other, resulting in an increase of C_B, and, hence, in a decrease of the rate of crystallization. Various approximations exist for estimating this effect. For a motionless system at a constant temperature, a useful approximation is known as the Kolmogorov–Mehl–Johnson–Avrami equation [18],

$$\frac{C_0-C}{C_0-C_i}=\exp\left[-(k_At)^n\right] \tag{3}$$

where k_A is the rate coefficient, and n is the Avrami exponent.

Fig. 6 demonstrates that Eq. (3) is indeed en excellent approximation of the observed behavior of spinel over a wide range of time and temperatures [19]. The lines in Fig. 6 represent Eq. (3) with Eq. (2) for C_0 and the Arrhenius function for k_A:

$$k_A=k_{A0}\exp(-B_A/T) \tag{4}$$

where k_{A0} and B_A are temperature-independent coefficients. A similar diagram was constructed for nepheline [17] and aegirine (acmite) [15].

Eq. (3) cannot be used for a nonisothermal situation. By the principle of frame-independence, the rate can only be a function of the frame-independent variables, which excludes time. A frame-indifferent differential equation that yields Eq. (3) for $T=$ const. has the form [8,20]

$$\frac{dC}{dt}=nk_A(C_0-C)\left[-\ln\left(\frac{C_0-C}{C_0-C_i}\right)\right]^{(n-1)/n} \tag{5}$$

Other kinetic equations originally developed for isothermal situations were modified in a similar fashion [21].

For a constant cooling rate, $dT/dt=-\Phi$, i.e., with $dC/dt=-\Phi dC/dT$, and Eq. (5) can be solved numerically if k_A and C_0 are known as functions of T—such as those given by Eqs. (2) and (4). A solution for spinel precipitation in a waste glass is displayed in Fig. 7 as C versus t and C versus T with Φ as a parameter [8]. As expected, a fast cooling rate produces little crystallinity, whereas an extremely slow cooling rate results in nearly equilibrium crystallinity.

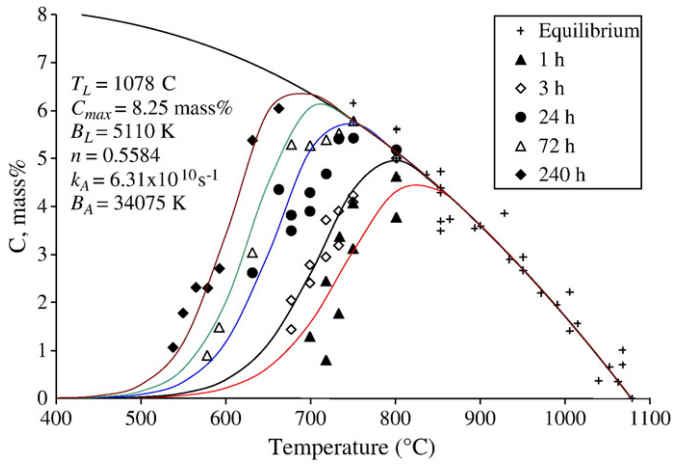

Fig. 6. Spinel fraction, in mass%, versus temperature and time (a parameter) during isothermal heat treatment of a simplified nuclear waste glass. The lines represent Eqs. (2)–(4) fitted to data.

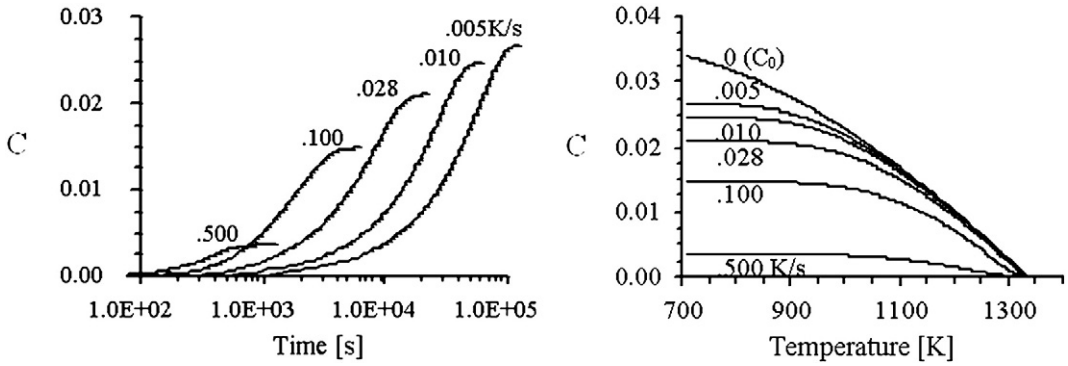

Fig. 7. Spinel concentration (as a mass fraction) versus time and temperature during cooling at a constant rate.

Fig. 8 shows an alternative representation known as a time–temperature transformation diagram in which the C is mapped on a T–t plane. This diagram is valid solely for the cooling represented by a linear function $T = T_L - \Phi t$, where t is measured from the moment at which the decreasing temperature (at a constant rate, Φ) reached T_L. Note: if constructed from isothermally obtained data, conclusions drawn from such a diagram for nonisothermal crystallizations are potentially misleading.

When the melt flows or crystals move, the diffusion layers are suppressed, and the bulk concentration changes. This situation is addressed by the Hixson–Crowell Equation [22],

$$\frac{da}{dt} = 2n_S k_H \left(a_0^3 - a^3\right) \tag{6}$$

where k_H is the rate coefficient. Eq. (6) describes crystal dissolution or growth under hindered-settling conditions when densely populated crystals fall in otherwise quiescent melt unless they are so small that their velocity has a negligible effect on the bulk melt flow [19].

Using the boundary layer theory, Levich derived an equation for the concentration boundary layer of a dissolving falling crystal [23]:

$$\delta = \frac{1.15\left(\frac{\theta - \sin 2\theta}{2}\right)^{1/3}}{\sin\theta}\left(\frac{Da^2}{3u}\right)^{1/3} \tag{7}$$

where θ is an angular coordinate, and u is the velocity. This equation was verified with the images of spinel crystals falling in the melt held at a temperature above the liquidus [13]. As seen in Fig. 9, the crystals were leaving behind a comet-like tale of colored glass, the shape of which was well described by Eq. (7). Moreover, the measured horizontal concentration distribution and dissolution rate resulted in a value of D similar to that found in the literature [24].

The rate of growth and dissolution of spinel crystals is plotted in Fig. 10 as a function of temperature [13]. As the temperature increases, the growth rate increases to a maximum and then decreases to zero at T_L. Similar curves were obtained for other systems—see, e.g., [25]. Note that the dissolution rate does not drop to zero at T_L because crystals can dissolve at $T < T_L$ if $C > C_0$.

6. Effect of crystallization on nuclear-waste-glass processing and on the waste-glass quality

Crystal formation may interfere with glass processing and glass quality. Here we discuss crystal settling in the melter, precipitation of crystals in the canister, and the effect of crystallization on the waste-glass chemical durability.

Crystal settling is a potential problem regarding the performance and even the lifetime of a continuous waste-glass electric melter [26]. Spinel crystals that grow in the batch and reach the melt circulating in the melter are carried to the vicinity of the melter bottom where they can settle and form a growing layer of sludge. Eq. (6) with $k_H = k_{H0}\exp(-B_H/T)$, where k_H and B_H are temperature-independent coefficients, was used in a mathematical model that estimated the distribution of spinel in the melter, both with respect to its crystal size and the mass fraction, and the sludge layer growth rate as a function of position on the melter bottom [27].

The most important parameter that affects the sludge layer growth is the crystal size. This can be demonstrated with a simple calculation [26]. The rate of growth of the sludge layer is $U = uv_G/v_S$, where u is the Stokes

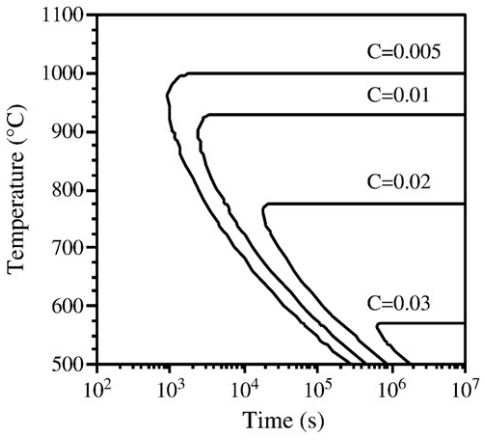

Fig. 8. Time–temperature transformation plot for spinel precipitating from molten glass at a constant rate of cooling. This diagram presents the same relationship as those in Fig. 7.

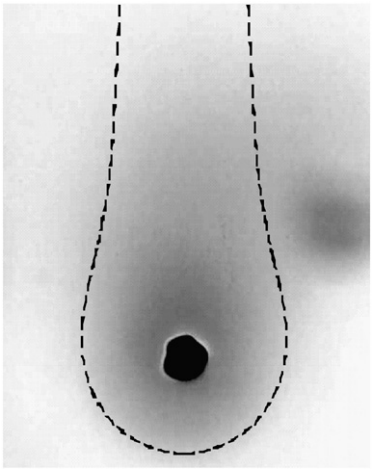

Fig. 9. An optical micrograph of a falling and dissolving crystal of spinel (~20 μm in diameter) in a simplified simulated nuclear waste glass.

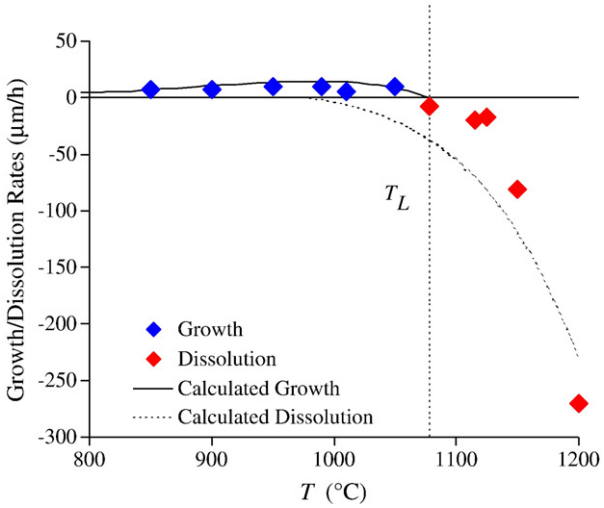

Fig. 10. Growth and dissolution rate of spinel in a simplified simulated nuclear waste glass versus temperature.

velocity, and v_G and v_S are the spinel volume fraction in glass and in sludge, respectively. By the Stokes equation, $u = k_S \Delta\rho g a^2/\eta$, where k_S is the Stokes coefficient ($k_S = \sim 0.04$ for hindered settling of octahedrons [28]), $\Delta\rho$ is the density difference between spinel and melt, g is the acceleration due to gravity, and η is the melt viscosity. With $\Delta\rho \approx 2.5 \times 10^3$ kg m^{-3}, $g \approx 10$ m s^{-2}, $\eta \approx 10$ Pa s, and $a \approx 10^{-4}$ m, we obtain $u \approx 1.3 \times 10^{-6}$ m s^{-1} and with $a \approx 10^{-6}$ m, $u \approx 5 \times 10^{-10}$ m s^{-1}. Based on samples from experimental melter runs, $v_S = \sim 0.15$. With $v_G = 0.005$, we estimate $U \approx 3 \times 10^{-8}$ m s^{-1} for 100-μm crystals and 3×10^{-12} m s^{-1} for 1-μm crystals. Hence, 100-μm crystals would create 0.9-m sludge in 1 year in this extreme case. Spinel agglomerates would settle even faster. On the other hand, small crystals may totally dissolve while circulating in the melter. Even in the worst case of no dissolution, crystals of ~1 μm in size are likely to be discharged from the melter with glass, leaving behind a minute 95-μm layer of sludge in 1 year.

Spinel sludge, when formed, cannot be dissolved within a reasonable length of time because the melter bottom is relatively cold, and the sludge cannot be easily disturbed [29]. Fig. 11 shows an optical micrograph of a thin section of a spinel sludge, the sample of which was retrieved from an experimental melter vitrifying simulated waste made without adding the noble metals [30]. Spinel crystals grew large (~100 μm) and produced a layer of sludge within a relatively short melter run. Even more worrisome is the possibility of spinel settling within the melter discharge zone during the time of melter idling. Here not only the crystal size is important, but also

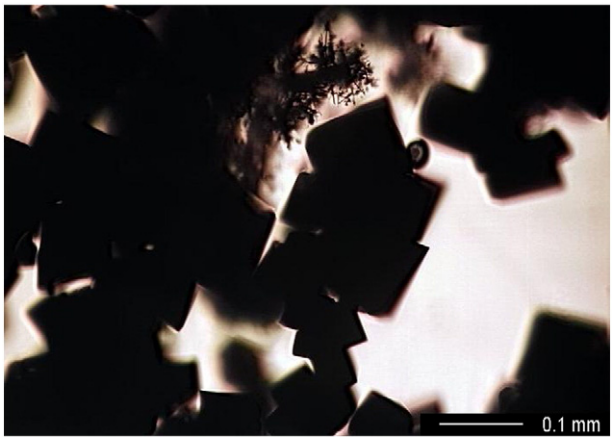

Fig. 11. Optical image of a thin section through a spinel sludge taken from an experimental waste glass melter (the dendrites in the middle top are metallic silver).

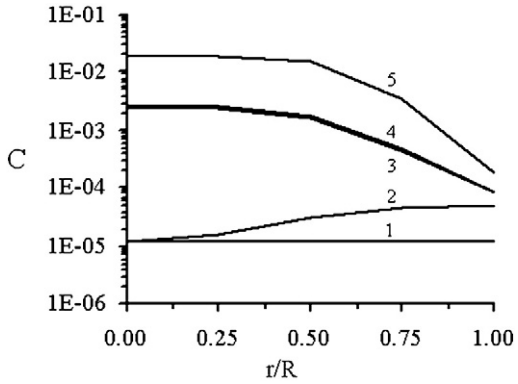

Fig. 12. Spinel volume fraction versus radial coordinate, r, in the cylindrical canister of the internal radius R at the ends of the five stages described in the text.

the T_L; crystallinity can be eliminated if the temperature in the discharge zone is kept above the liquidus.

To decrease the crystal size to 1 μm, it is necessary to increase n_S from 10 mm^{-3} to 10^7 mm^{-3}. This can be achieved with good nucleation agents. As Fig. 5 indicates, n_S becomes large when noble metals are present in the waste [15]. In nuclear wastes, Ru, Rh, and Pa are common minor components [6].

Crystals of RuO_2 can also form sludge, with or without spinel. Needles of RuO_2 not only increase the resistance of the sludge against mechanical agitation, but also can distort the electric field in the melter because RuO_2 is electrically conductive [31]. When mathematical modeling was applied to the settling of RuO_2 crystals [32], the model predicted that needles of RuO_2 cannot settle during the melter life time in any measurable amount. This, however, was at variance with pilot-scale experiments. The authors resolved the paradox by assuming that the crystals that come to some distance from the melter bottom are somehow trapped. The entrapment distance necessary for an agreement with experiment would be several times larger than the crystal size. The authors did not explain how this would be possible. However, as RuO_2 crystals are known to form agglomerates [31,33–35] (an effect of densification in the shrinking pockets of molten salts during melting and the shear-flocculation mechanism in the circulating melt [34]), the enhanced settling is probably a result of higher sinking velocity of the agglomerates. Even though the density of the

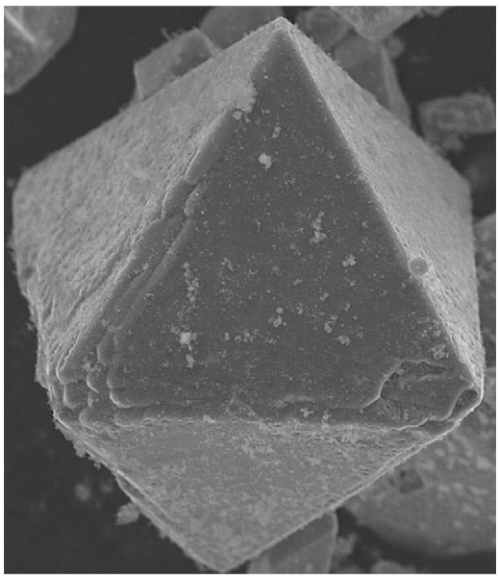

Fig. 13. A typical octahedron of a spinel crystal in a simulated nuclear waste glass. The octahedron edges are 55 μm long.

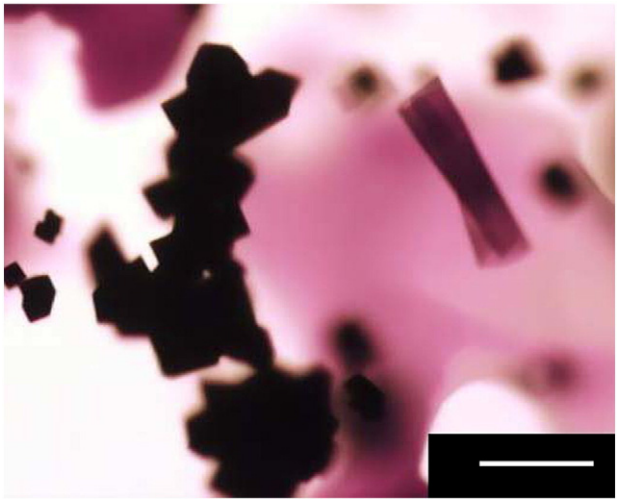

Fig. 14. An aggregate of spinel crystals in a simulated nuclear waste glass and a 100-μm bar.

agglomerates is lower than the density of crystals, their sizes can be sufficiently large to substantially increase the settling velocity.

Waste glass is discharged from the melter into canisters in which it cools at a relatively slow rate of ~0.05 K/s in the centerline. The full time–temperature history of a glass poured from the melter discharge to a canister of 60 cm in diameter and 2 m long can be viewed as consisting of five stages [8]: 1) the stream of the melt falls from the melter discharge to the canister opening, 2) the melt flows from the point of impact towards the canister wall, 3) the melt rests on the top surface of the glass in the canister, 4) the top melt is covered by the subsequent layer, and 5) the glass cools down. Combined Eqs. (2), (4), and (5) were used to estimate the spinel fraction distribution shown in Fig. 12.

Crystallization affects the chemical durability of glass by changing the composition of the matrix glass in which they are embedded. The average composition of the glass phase can thus be obtained from the fraction and composition of the crystalline phases present and the chemical durability can be estimated with mathematical models [36]. However, other effects can increase the corrosion rate, such as the existence of diffusion layers around the crystals (these layers are more depleted of the crystal-forming components than the bulk glass), internal stresses associated with crystallization, the presence of cracks caused by internal stresses, water diffusion around the interfaces, crystallization-induced phase separation, etc. Fortunately, for the lack of nucleation, a long incubation time, and a slow growth, most of the crystalline forms do not actually occur during glass cooling, or they form in concentrations too low to influence the rate of glass corrosion. The notable exception is nepheline that readily forms below T_L and its precipitation does not stop at the glass-transition temperature (T_g) the of the original glass because the T_g of the matrix glass decreases, as nepheline, $NaAlSiO_4$, is depleting it from the glass-network units SiO_4 and AlO_4 [17].

7. Dendritic growth

The common shapes of crystals formed during slow cooling or at a constant temperature not far below the T_L are compact and determined by the particular crystallographic group. Thus, spinel forms regular octahedrons (Fig. 13) that may group into agglomerates (Fig. 14). Nepheline and baddeleyite crystals are displayed in Fig. 15. If the melt is subjected to rapid cooling to a temperature at which the rate of growth is fast, the moving interface breaks through the thin diffusion layer, creating instability that leads to the formation of dendrites [37], as seen in Fig. 16 [30].

8. Self-organization phenomena

Spinel crystals may organize themselves into layers, as seen in Fig. 17 [38]. These layers are often bent and distorted by convection or by moving bubbles. They are a manifestation of the Liesegang phenomenon [39,40]. When the temperature gradient moves through the melt, spinel crystallizes when the temperature decreases below T_L, and the diffusion of spinel components depletes the melt from them up to some distance. The new layer begins to crystallize when the moving T_L front reaches the undepleted mass. This can happen during cooling, for example, when the melt is poured from a crucible on a cold steel. This can also happen during reheat, for example, when the stream of the hot melt flows over a colder melt [38]. Both dendritic growth and the Liesegang effect have been well understood and mathematically described in the literature [37,39,40].

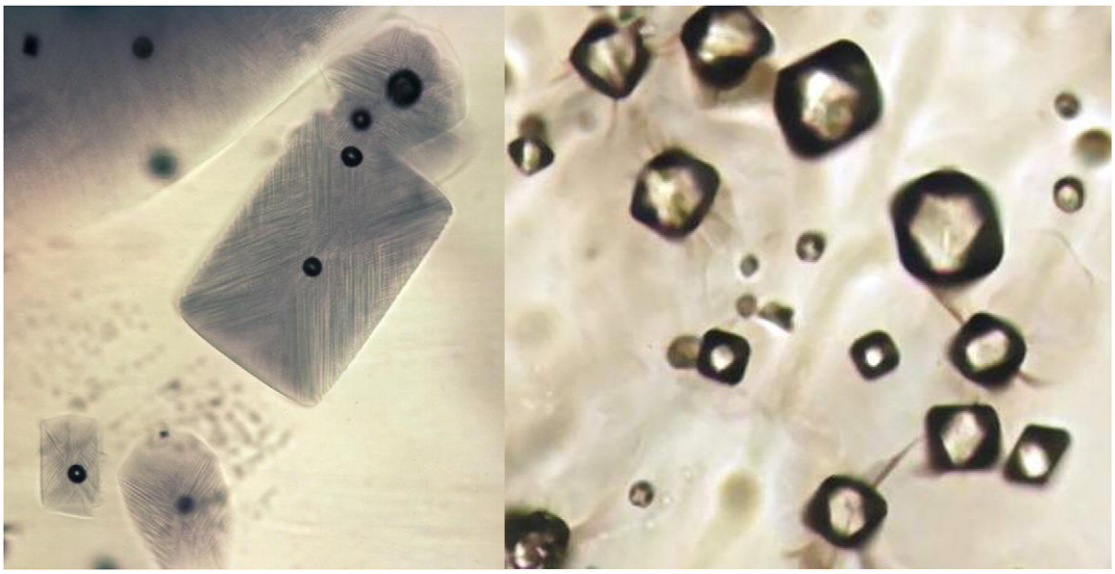

Fig. 15. Crystals of nepheline ($NaAlSiO_4$), left, and baddeleyite (ZrO_2), right, in a simulated nuclear waste glass. The large nepheline crystal is 200 × 300 μm and the two large baddeleyite crystals are ~75 μm in size.

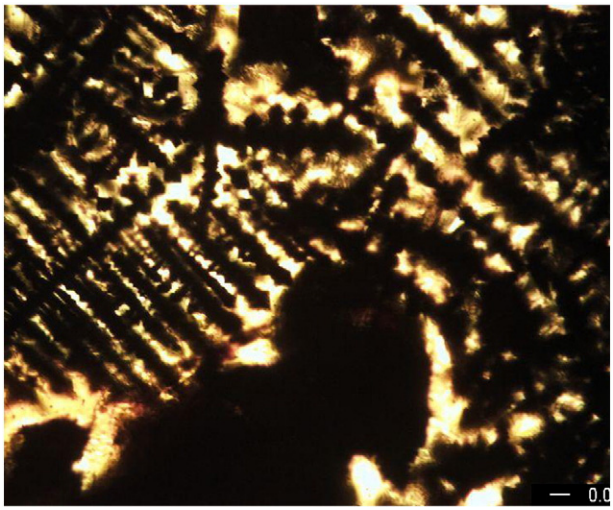

Fig. 16. Spinel dendrites in a simulated nuclear waste glass.

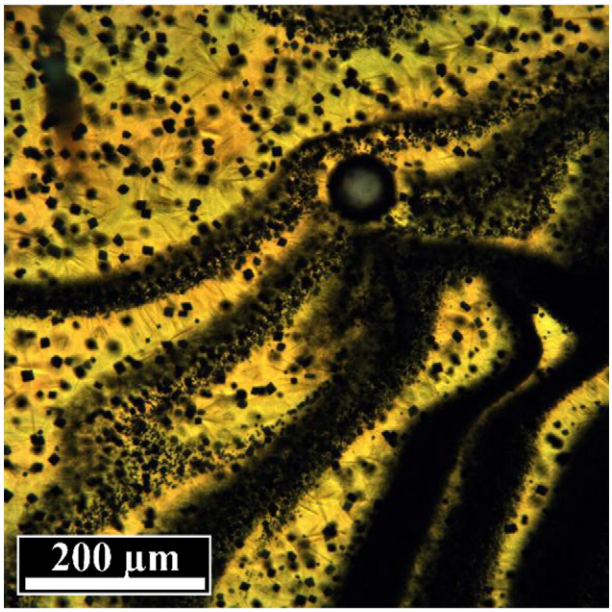

Fig. 17. Spinel crystals in a simulated nuclear waste glass poured into a canister. Large crystals nucleated during pouring, and the small crystals, self-organized into layers (here disturbed by a moving bubble), formed when hot glass reheated a cooler glass below.

9. Conclusions

Crystal growth and dissolution occurs during continuous processing of commercial glasses and is common in melting of nuclear waste glasses. Under these circumstances, crystal nucleate, grow, and dissolve commonly in highly multicomponent glasses where non-isothermal conditions and deformation/flow cannot be ignored. Therefore, the rate equation is of the form $dC/dt = f(C,T)$ where 1) both thermodynamic and kinetic parameters (the equilibrium concentration and the rate coefficient) are treated as functions of temperature and 2) the convective diffusion is taken into account. Dendritic crystal growth and self-organization of crystals into Liesegang bands add to the process complexity.

Acknowledgments

Illustrations used in review are mainly based on published work of my colleagues and students interns. Just to name a few: Jessie Alton, Dan Casler, Jarrod Crum, Milos Jiricka, Pepa Matyas, Trevor Plaisted, Brian Riley, Mike Schweiger, John Vienna, and Ben Wilson. The author is grateful to the U.S. Department of Energy Office of River Protection for support of this review. Pacific Northwest National Laboratory (PNNL) is operated for the U.S. Department of Energy by Battelle under Contract DE-AC05-76RL01830.

References

[1] M. Cable, Glass: Science and Technology, in: D.R. Uhlmann, N.J. Kreidl (Eds.), Academic Press, 1984.
[2] R.G.C. Beerkens, in: H. Loch, D. Krause (Eds.), Mathematical Simulation in Glass Technology, Springer, 2002.
[3] R.G.C. Beerkens, Silikaty 52 (2008) 206.
[4] P. Hrma, Adv. in Fusion of Glass, 10, Am. Ceram. Soc, Westerville, Ohio, 1988, pp. 1–18.
[5] P. Hrma, in: A. Paul (Ed.), Chemistry of Glass, Prentice Hall, London, 1990.
[6] P. Izak, P. Hrma, B.W. Arey, T.J. Plaisted, J. Non-Cryst. Solids. 289 (2001) 17.
[7] P. Hrma, J. Matyáš, D.-S. Kim, 9th Biennial Int. Conf. On Nucl. Hazardous Waste Management, Spectrum '02, American Nuclear Society, CD-ROM, 2002.
[8] D.G. Casler, P. Hrma, Mat. Res. Soc. Proc. 556 (1999) 255.
[9] P. Hrma, D.E. Smith, J. Matyáš, J.D. Yeager, J.V. Jones, E.N. Boulos, Europ. J. Glass Sci. Technol. B. 47 (2006) 64.
[10] P. Hrma, A.A. Kruger, Advanced Materials Research, 633, 2008, pp. 39–40, online at http://www.scientific.net.
[11] B. Hanni, E. Pressley, J.V. Crum, K.B.C. Minister, D. Tran, P. Hrma, J.D. Vienna, J. Mater. Res. 20 (2005) 3346.
[12] J.D. Vienna, A. Fluegel, D.S. Kim, P. Hrma, Glass Property Data and Models for Estimating High-Level Waste Glass Volume, PNNL-18501, Pacific Northwest Laboratory, Richland, Washington, 2009.
[13] J. Alton, T.J. Plaisted, P. Hrma, J Non-Cryst. Solids 311 (2002) 24.
[14] J.D. Vienna, P. Hrma, J.V. Crum, M. Mika, J. Non-Cryst. Solids 292 (2001) 1.
[15] D. Vienna, P. Hrma, D.E. Smith, in: W.J. Gray, I.R. Triay (Eds.), Scientific Basis for Nuclear Waste Management, 465, 1997, p. 17.
[16] J.H. Li, P. Hrma, J.D. Vienna, M. Qian, Y. Su, D.E. Smith, J. Non-Cryst. Solids 311 (2003) 202.
[17] T.J. Menkhaus, P. Hrma, H. Li, Ceram. Trans. 107 (2000) 461.
[18] M. Avrami, J. Chem. Phys. 7 (1939) 1103; 8 (1940) 212; 9 (1941) 177.
[19] J. Alton, T.J. Plaisted, P. Hrma, Chem. Engn. Sci. 57 (2002) 2503.
[20] D.W. Henderson, J. Non-Cryst. Solids 30 (1979) 17.
[21] A.S. Sinitskii, V.A. Ketsko, G.P. Murav'ea, N.N. Oleynikov, Rus. J. Inorg. Chem. 49 (2004) 1001.
[22] A.W. Hixson, J.H. Crowell, Ind. Eng. Chem. 23 (1931) 923.
[23] V.G. Levich, Physicochemical Hydrodynamics, Prentice-Hall, New York, 1962, p. 80.
[24] M.P. Borom, J.A. Pask, J. Am. Ceram. Soc. 51 (1968) 490.
[25] S. Reinsch, M.L.F. Nascimento, R. Müller, E.D. Zanotto, J. Non-Cryst. Solids 354 (2008) 5386–5394.
[26] P. Hrma, J. Alton, J. Klouzek, J. Matyas, M. Mika, L. Nemec, T.J. Plaisted, P. Schill, M. Trochta, Waste Manag. '01, University of Arizona, Tucson, Arizona, 2001.
[27] P. Schill, M. Trochta, J. Matyas, L. Nemec, P. Hrma, Waste Management '01, University of Arizona, Tucson, Arizona, 2001.
[28] J. Klouzek, J. Alton, T.J. Plaisted, P. Hrma, Ceram. Trans. 119 (2001) 301.
[29] M. Mika, P. Hrma, M.J. Schweiger, Ceram. Silik. 44 (2000) 86.
[30] M. Jiricka, P. Hrma, Ceram. Silik. 46 (2002) 1.
[31] G. Roth, S. Weisenburger, Role of Noble Metals in Electrically Heated Ceramic Waste Glass Melters, Forschungscentrum Karlsruhe Institut für Nucleare Entforschung, Karlsruhe, Germany, 2003.
[32] W. Lutze, W. Gong, F.C. Perez-Cardenas, K.S. Matlack, I.L. Pegg, P. Schill, Europ. J. Glass Sci. Technol. A 48 (2007) 263;
P. Schill, W. Lutze, W. Gong, I. Pegg, Europ. J. Glass Sci. Technol. A 48 (2007) 276.
[33] C. Krause, B. Luckscheiter, J. Mat. Res. 6 (1991) 2535.
[34] W.T. Cobb, P. Hrma, Ceram. Trans. 23 (1991) 233.
[35] M.F. Cooper, M.L. Elliott, L.L. Eyler, C.J. Freeman, J.J. Higginson, L.A. Mahoney, M.R. Powell, Research-scale Melter Test Report, PNL-9428, Pacific Northwest Laboratory, Richland, Washington, 1994.
[36] B.J. Riley, P. Hrma, J.A. Rosario, J.D. Vienna, Ceram. Trans. 132 (2002) 257.
[37] M.H. Burden, J.D. Hunt, J. Crystal Growth 22 (1974) 109.
[38] M.J. Schweiger, M.W. Stachnik, P. Hrma, Ceram. Trans. 87 (1998) 335.
[39] K.H. Stern, Chem. Rev. 54 (1954) 79.
[40] P. Ortoleva, in: G. Nicolis, F. Baras (Eds.), Chemical Instabilities, 1984, p. 289, Kluwer, Dordrecht.